Repurposing dihydroartemisinin as a novel anticancer agent against colorectal cancer stem cells

Recommended Citation

Repurposing dihydroartemisinin as a novel anticancer agent against colorectal cancer stem cells

Meng-Han Wu [a], Chieh-Ju Sung [a], Fan-Lu Kung [a], Jih-Hwa Guh [a], Yeu Su [b], Lih-Ching Hsu [a,*]

[a] School of Pharmacy, National Taiwan University, Taipei 10050, Taiwan
[b] Institute of Biopharmaceutical Sciences, School of Pharmaceutical Sciences, National Yang Ming Chiao Tung University, Shi-Pai, Taipei 11221, Taiwan

Abstract

Colorectal cancer (CRC) is one of the leading causes of cancer-related death globally and discovering novel therapeutic agents to treat the disease, and prevent cancer metastasis and recurrence is an urgent medical need. Cancer stem cells (CSCs) capable of self-renewal and differentiation are generally considered the cause of tumor metastasis, recurrence and chemoresistance. Hence, targeting CSCs may be a promising strategy for the treatment of cancer. GATA6, a zinc finger transcription factor, contributes to tumorigenesis in CRC and is related to cancer stemness. GATA6-overexpressing stable clones OE4 and OE6 derived from HCT116 cells were previously established and exhibited increased stemness properties. In this study, we found that OE4 and OE6 cells displayed CSC-like properties, including higher expression levels of stemness-related proteins, increased sphere forming capacity and resistance to 5-fluorouracil. OE4 and OE6 cells also showed increased glucose uptake capacity, another hallmark of CSCs. Therefore, these two cell clones were employed as a CSC-like cell model to search for potential colorectal CSC-targeting drugs. Among several compounds tested, dihydroartemisinin (DHA), an antimalarial drug, exerted better anticancer activity toward OE4 and OE6 relative to the empty vector-transfected HCT116 cells. DHA also inhibited sphere formation and impaired glucose metabolism. DHA induced G0/G1 arrest and apoptosis. Moreover, DHA also induced reactive oxygen species and mitochondrial membrane potential loss. Thus, DHA caused mitochondrial damage which was confirmed by Seahorse mitochondrial stress test. DHA also increased LC3B-II and PINK1 protein levels, indicative of autophagy/mitophagy. In conclusion, repurposing DHA may be a potential strategy against colorectal CSCs and further validation using *in vivo* models is warranted.

Keywords: Autophagy/mitophagy, Colorectal cancer stem cells, Dihydroartemisinin, GATA6, Glucose metabolism

1. Introduction

According to GLOBOCAN 2022, colorectal cancer (CRC) ranks third in cancer incidence and is the second leading cause of cancer-related death for both sexes globally [1]. The 5-year survival rate is estimated to be ~90% for early-stage, but drops below 20% for metastatic CRC according to the American Cancer Society's survey [2]. Treatment options include surgical removal of tumor mass, radiation therapy, and chemotherapy such as fluoropyrimidine-based therapy. Targeted therapy and immunotherapy are also available for a subset of CRC patients [3].

Cancer stem cells (CSCs) are stem cell-like populations in tumors with self-renewal capacity. CSCs are quiescent and able to regenerate cancer cells; therefore, considered to be responsible for treatment failure and cancer recurrence. Thus, targeting CSCs may be a promising strategy to combat cancer and may provide a hope for cancer cure [4].

GATA6, a zinc finger containing transcription factor, is important for normal colonic epithelial differentiation and stem cell expansion [5]. Previous

studies have shown that overexpression of GATA6 is associated with colorectal tumorigenesis [6]. Furthermore, overexpression of GATA6 in a human CRC cell line HCT116 resulted in elevated mRNA levels of stem cell markers such as Oct4 and Nanog, and increased $CD44^+/CD133^+$ CSC populations and self-renewal ability [7]. Therefore, HCT116 cell clones overexpressing GATA6 could serve as a CSC-like cell model for the search of drugs that can target CSCs.

It has been reported that some CSCs exhibit significant aerobic glycolysis characteristics, such as, increased expression of glycolytic enzymes and increased production of lactic acid [8], suggesting that they may rely on more glucose supply for survival. It has also been demonstrated that targeting the facilitative glucose transporter GLUT1 using WZB117, a GLUT1 inhibitor, can inhibit the self-renewal and tumor-initiating capacity of pancreatic, ovarian and glioblastoma CSCs at lower doses than those required for inhibition of cancer cells growing in monolayers [9]. Overexpression of active glucose transporters SGLT1 and SGLT2 may provide cancer cells with the advantage of taking up glucose even under low glucose supply in tumor microenvironment and selective SGLT2 inhibitors such as dapagliflozin and canagliflozin have been reported to display anticancer activity [10].

Artemisinin, a well-known antimalarial drug, was discovered by Dr. Youyou Tu's research team in 1972 [11]. Apart from antimalarial activity, artemisinin has been reported to exhibit anticancer activity. However, the application in cancer therapy is limited due to poor solubility, short half-life and low bioavailability [12]. Dihydroartemisinin (DHA), a reduced lactol derivative of artemisinin, is more stable and much more potent than artemisinin in antimalarial activity [11]. DHA also shows anticancer activity in a wide variety of cancers including colorectal cancer [12]. The possible mechanisms of antitumor activity include induction of cell cycle arrest, apoptotic cell death, autophagy and ferroptosis, and inhibition of angiogenesis, cancer cell proliferation, metastasis and invasion [12,13]. Moreover, it has been reported that DHA can induce cell cycle arrest and apoptosis in glioma stem cells [14], however, related studies on CSCs remain limited. Artemisinin and its bioactive derivatives contain an endoperoxide moiety which is considered important for their antimalarial and anticancer activities. The endoperoxide bridge can be reduced by heme or free ferrous ion to produce free radicals or reactive oxygen species (ROS), which play an important role in the induction of cell death [12,13].

In this study, we used HCT116 cell clones overexpressing GATA6 as a CSC-like cell model to test whether GLUT1 or SGLT2 inhibitors, or DHA displayed anti-CSC activity, and found that DHA was effective against colorectal CSC-like cells. The potential underlying mechanisms were also investigated.

2. Materials and methods

2.1. Chemicals

DHA and canagliflozin were obtained from TargetMol, 2-NBDG, geneticin, propidium iodide (PI) and JC-1 dye were obtained from Invitrogen Life Technologies. Chloroquine, cisplatin, $2',7'$-dichlorodihydrofluorescein diacetate (DCFH-DA), 5-fluorouracil (5-FU), hydrogen peroxide (H_2O_2), WZB117, sulforhodamine B (SRB) and trichloroacetic acid (TCA) were obtained from Sigma-Aldrich. Stock solutions of DHA, 5-FU, canagliflozin, DCFH-DA, JC-1 and WZB117 were prepared in DMSO. Cisplatin, geneticin and TCA were dissolved in PBS. 2-NBDG and chloroquine were dissolved in ddH_2O. SRB solution was prepared in 1% acetic acid.

2.2. Cell culture, drug treatment and cell viability assay

The CRC cell line HCT116 was purchased from American Type Culture Collection and cultured in RPMI 1640 medium supplemented with 10% fetal bovine serum (FBS), 2 mM L-glutamine, and antibiotics (100 U/mL penicillin, 100 μg/mL streptomycin, and 0.25 μg/mL amphotericin B). Stable clones derived from HCT116 were established as previously described [7] and maintained in culture medium containing 600 μg/mL geneticin. Cells were cultured at 37 °C in a humidified 5% CO_2 atmosphere.

To determine cell viability, ~4000 cells/well were seeded into 96-well plates and treated with indicated concentrations of compounds for 72 h, and then fixed with 10% TCA for the SRB assay. OD was measured with SpectraMax iD3 Paradigm Microplate Reader (Molecular Devices) at 515 nm. IC_{50} values were obtained from cell viability data using GraphPad Prism 8 software with curve-fitting.

2.3. Sphere formation assay

For the sphere formation assay, 2×10^4 cells/well were seeded in ultralow attachment 6-well plates (COSTAR, Corning Inc.) with serum-free RPMI 1640 medium supplemented with 1.25% N2 supplement, 20 ng/mL epidermal growth factor, 10 ng/mL basic fibroblast growth factor, 6 mg/mL glucose, 4 mg/mL

bovine serum albumin (BSA) and antibiotics [7]. Cells were treated with or without DHA for 7 days. Fresh serum-free medium and DHA were supplemented to each well on the fourth day of the 7-day treatment period. The number of spheres larger than 40 μm was counted and the image was captured with the OLYMPUS CKX41 microscope equipped with an OLYMPUS E-330 camera-ADU1.2x.

2.4. Western blot analysis

Cells were seeded in 6-well plates and treated with indicated compounds for 24 h (3×10^5 cells/6-well) and 48 h (2×10^5 cells/6-well), then harvested by trypsinization and lysed in RIPA buffer as described [15]. Protein concentration was determined by BCA protein assay (Thermo Fisher Scientific), and denatured lysates containing 30 μg total protein were subjected to SDS-PAGE followed by Western blot analysis. Primary antibodies used included Sox2, Oct 4, Nanog, GAPDH, PARP, LC3B, PINK1 (Gene-Tex), GATA6 (Santa Cruz Biotechnology), and γ-tubulin (Sigma). Secondary antibodies used were HRP-conjugated anti-mouse and anti-rabbit IgG (Cell Signaling Technology). γ-Tubulin or GAPDH was used as a loading control. Image detection and analysis were performed using the ChemiDoc MP system with Image Lab software (BioRad Laboratories).

2.5. Detection of the CD44⁺/CD133⁺ subpopulation by flow cytometry

To determine the CD44⁺/CD133⁺ subpopulation, HCT116 cells and GATA6-overexpressing OE4 cells cultured in 6-well plates were harvested by trypsinization, washed with cold PBS, then resuspended in FACS buffer (1% BSA and 0.1% sodium azide in PBS) and stained with FITC-conjugated CD44 and PE-conjugated CD133 (Miltenyi Biotech) for 1 h at 4 °C. Cells were then centrifuged at 300×g for 5 min at 4 °C, resuspended in 200 μL FACS buffer and subjected to flow cytometric analysis. Unstained control cells and HCT116 cells stained with a single antibody were included for adjusting fluorescence compensation and for defining the CD44⁺ or CD133⁺ subpopulation. The two-dimensional dot plot analysis was performed using FACSCalibur flow cytometer (Becton Dickinson), and data were analyzed with FlowJo software (Tree Star Inc.).

2.6. 2-NBDG uptake assay

The glucose uptake capacity was evaluated using 2-NBDG, a glucose analogue that can be transported by GLUTs. Cells seeded in a 6-well plate (2×10^5 cells/well) were treated with DMSO (vehicle control) or DHA for 48 h, then 200 μM 2-NBDG was added and incubated for 1.5 h. Cells were then harvested by trypsinization, suspended in 200 μL cold PBS, and 2-NBDG uptake was detected by flow cytometry [16]. Data were analyzed with FlowJo software and geomean of fluorescence intensity was used to calculate the relative glucose uptake capacity.

2.7. Detection of lactate levels

Lactate levels were determined using the L-lactate colorimetric assay kit (ab65330, Abcam). Cells were seeded in 12-well plates (5×10^4 cells/well) and treated with DHA for 48 h. Culture medium of each sample (100 μL) was collected in a microfuge tube and deproteinized with 35 μL 50% TCA. After incubation for 15 min on ice, samples were centrifuged at 12,000×g for 5 min at 4 °C. The supernatant (90 μL) was collected into another tube and 10 μL 30% KOH was added to neutralize the excessive TCA for 5 min on ice. Then, 1 μL sample was diluted with 49 μL lactate assay buffer and incubated with 2 μL probe and 2 μL enzyme mix at room temperature for 30 min, and OD was measured with SpectraMax iD3 Paradigm Microplate Reader at 570 nm.

2.8. Cell cycle analysis by PI staining and flow cytometric analysis

Cells were seeded in 6-well plates (1×10^5 cells/well), treated with 3 and 10 μM DHA for 24 and 48 h, then harvested by trypsinization, fixed with 70% ethanol, and subjected to PI staining and flow cytometric analysis using FACSCalibur. Cell cycle distribution was analyzed with FlowJo software.

2.9. Detection of ROS by DCFH-DA assay

Cells were seeded in 12-well plates (1×10^5 cells/well) and treated with 10 μM DHA for 8 and 24 h. DCFH-DA (10 μM) was added to the cells 30 min before termination of the incubation. H_2O_2 (100 μM) was added to cells 5 min before termination of DCFH-DA staining as a positive control for ROS induction. Cells were then harvested by trypsinization and suspended in cold PBS for flow cytometric analysis using FACSCalibur. Results were analyzed by FlowJo software.

2.10. Detection of mitochondrial membrane potential by JC-1 assay

Cells were seeded into 12-well plates (1×10^5 cells/well) and treated with 3 μM DHA for 24 and 48 h, and 5 μg/mL JC-1 dye was added to the cells 30 min before the termination of the incubation period. Cisplatin (80 μM) was added to cells 5 min before termination of JC-1 staining as a positive control for the induction of MMP loss. Cells were harvested by trypsinization, suspended in cold PBS, and subjected to flow cytometric analysis. Acquired data were analyzed by FlowJo software.

2.11. Mitochondrial stress test assay

Cells ($1.5−2.5 \times 10^4$ cells/well) were seeded in Seahorse XFe24 cell culture plates in RPMI 1640 supplemented with 10% FBS, 2 mM L-glutamine and antibiotics overnight, then treated with 3 μM DHA for 24 h. The culture medium was then switched to the assay medium, Seahorse XF RPMI medium (103576-100, Agilent) supplemented with 2 mM L-glutamine, 2 g/L D-glucose and 2% FBS. Mitochondrial stress was determined using Seahorse XFe24 Cell Mito Stress Test Kit (103015-100, Agilent). Mitochondrial modulators were diluted in the assay medium to final concentrations of 1 μM oligomycin, 1.2 μM FCCP and 0.5 μM antimycin A/rotenone. Oxygen consumption rate (OCR) was measured according to the manufacturer's protocol in a Seahorse XFe24 analyzer (Agilent). Results were displayed and analyzed by Seahorse Wave Controller Software 2.6 (Seahorse Bioscience) and normalized with the cell number.

2.12. Data analysis

Quantitative data are presented as mean ± SEM of at least three independent experiments. All data analyses were performed with Microsoft Office Excel 2019 software and GraphPad Prism 8. Statistical analysis of data was conducted using the two-tailed Student's *t*-test and *P* values less than 0.05 were considered statistically significant.

3. Results

3.1. GATA6-overexpressing HCT116 cells display cancer stem cell characteristics

We first characterized GATA6-overexpressing HCT116 stable cell clones OE4 and OE6 to verify the CSC-like cell model for CRC. The sphere forming capacity of OE4 and OE6 cell clones was significantly higher than that of the parental HCT116 cells or HCT116 cells stably transfected with an empty vector (Vec) (Fig. 1A), suggesting that self-renewal ability of these OE cells was much higher than the parental HCT116 cells and Vec, which exhibited similar properties, therefore, only one of them was used as a control in some of the following studies.

In addition to sphere formation, transcription factors involved in stemness maintenance, such as Sox2, Oct4, and Nanog, are also widely used to assess the CSC-like properties. As shown in Fig. 1B, relative protein levels of Sox2, Oct4, and Nanog in OE4 and OE6 cell clones were higher than Vec. CSCs are generally considered the main cause of therapy resistance in CRC [17]. As shown in Fig. 1C, the 50% inhibitory concentration (IC_{50}) values of 5-FU, a standard chemotherapeutic agent for CRC, in OE4 and OE6 cells (9.44 and 9.94 μM respectively) were indeed significantly higher than that in Vec (5.07 μM). Moreover, CD44 and CD133 are considered the surface markers of colorectal CSCs. As shown in Fig. 1D, the $CD44^+/CD133^+$ population in OE4 cells was profoundly higher than that in HCT116 cells.

Taken together, the GATA6-overexpressing HCT116 stable cell clones OE4 and OE6 can be used as a colorectal CSC-like cell model.

3.2. DHA selectively targets colorectal CSC-like cells and the action of DHA is associated with glucose metabolism

It has been reported that targeting the facilitative glucose transporter GLUT1 using a GLUT1 inhibitor WZB117 may be an effective strategy to interrupt the tumor-initiating capacity and self-renewal potential of CSCs [9]. Furthermore, selective SGLT2 inhibitors for treatment of type 2 diabetes, such as dapagliflozin and canagliflozin, have been reported to exhibit anticancer activity [10]. DHA, a well-known antimalarial drug, has also been shown to display anti-CSC activity [13,14]. Therefore, canagliflozin, WZB117 and DHA were selected as potential colorectal CSC-targeting agents and tested in our verified CSC-like cell model using the SRB assay. As shown in Fig. 2A, the IC_{50} values of canagliflozin in OE4 and OE6 were significantly higher than in Vec, while the IC_{50} of WZB117 in Vec, OE4 and OE6 were all above 30 μM. In contrast, the IC_{50} values of DHA in OE4 and OE6 were much lower than in Vec cells, indicating that DHA differentially targeted colorectal CSC-like cells.

Sphere formation assay was also conducted to investigate the effect of DHA on self-renewal capacity. As illustrated in Fig. 2B, using
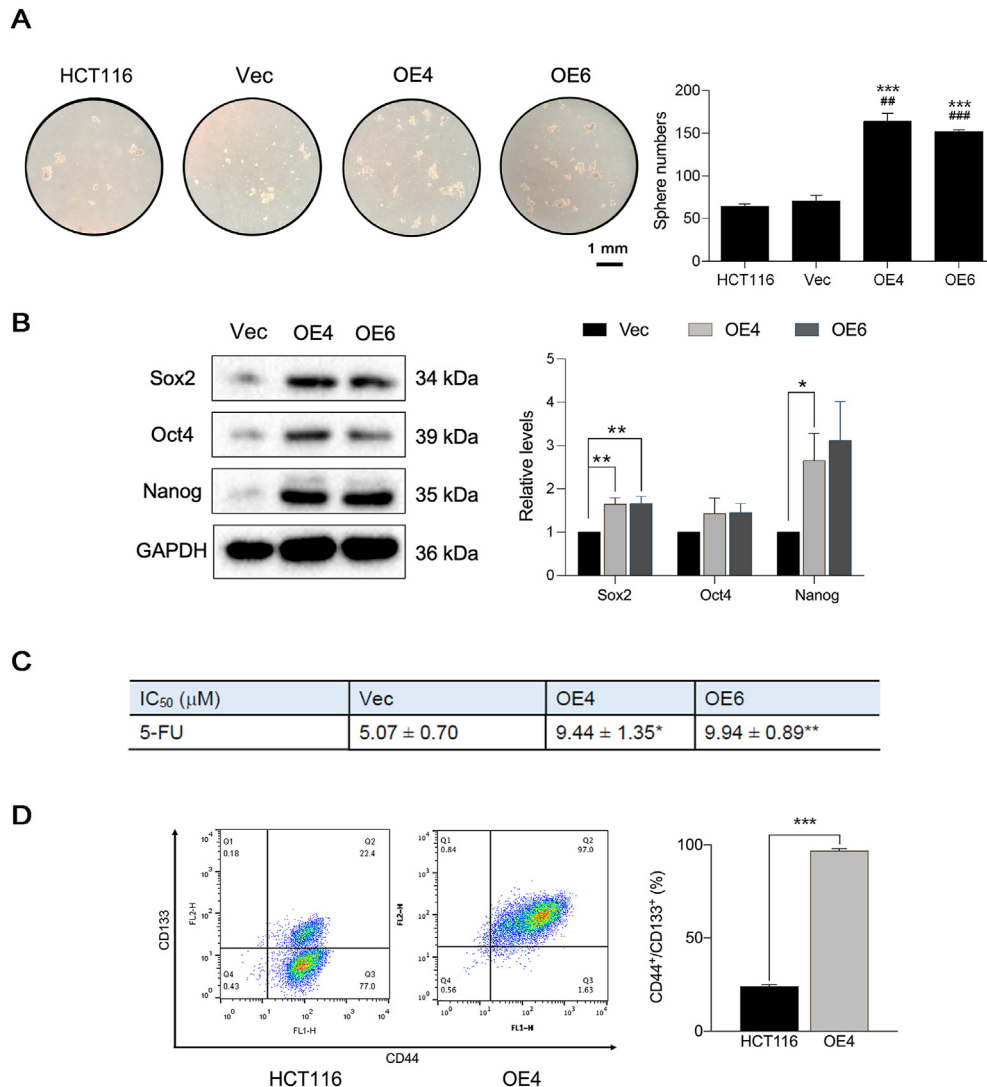
Fig. 1. HCT116 stable clones overexpressing GATA6 exhibit cancer stem cell-like characteristics. (A) Representative images and quantitative results of sphere formation assays in HCT116, HCT116 stably transfected with an empty vector (Vec), OE4 and OE6 cells. ***P < 0.001 vs. HCT116; ##P < 0.01, ###P < 0.001 vs. Vec. All images were captured at a magnification of 40 × . Scale bar: 1 mm. (B) Western blot analysis and quantitative results of stem cell markers Sox2, Oct4 and Nanog in Vec, OE4 and OE6 cells. (C) IC$_{50}$ values of 5-FU in Vec, OE4 and OE6 cells. The SRB assay was performed after 72 h of 5-FU treatment to determine cell viability and calculate IC$_{50}$ values. (D) Representative plots and quantitative results of HCT116 and OE4 cells stained with surface markers CD44 and CD133. *P < 0.05, **P < 0.01, ***P < 0.001.

concentrations equivalent to IC$_{50}$ values obtained by the SRB assay, DHA only inhibited sphere formation in HCT116 and Vec from 64.7 to 70.7 to 47.0 and 49.3 spheres, corresponding to 27.4% and 30.3% inhibition, but markedly decreased sphere formation in OE4 and OE6 cells from 163.7 to 152.0 to 74.7 and 73.7 spheres, corresponding to 54.4% and 51.5% inhibition.

Studies have unveiled that some types of CSCs highly rely on aerobic glycolysis, and glucose metabolism is associated with stemness maintenance of these CSCs [8,9]. To investigate possible targeting mechanisms of DHA, 2-NBDG uptake assay coupled with flow cytometry was conducted to

determine the glucose uptake capacity. The relative glucose uptake capacity of OE4 and OE6 clones was significantly higher than that of Vec, but significantly impaired after 48 h of treatment with DHA (Fig. 2C).

Lactate, the end product of glycolysis, was produced at higher levels in OE4 and OE6 cells than in HCT116 cells as revealed by measuring the extracellular lactate (Fig. 2D), suggesting that the glycolytic activity of CSC-like cells was higher than HCT116 cells. DHA not only impaired glucose uptake but also interrupted glycolysis as the relative lactate production level in OE4 cells was reduced dose-dependently by DHA after 48 h of treatment (Fig. 2E).

A

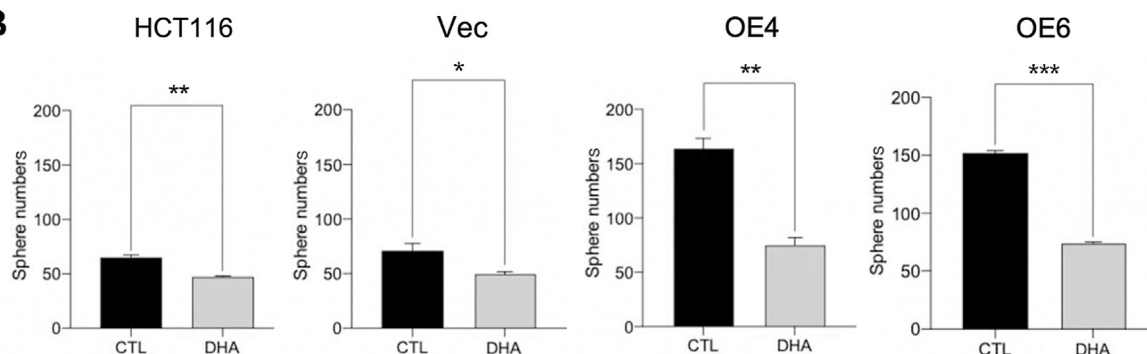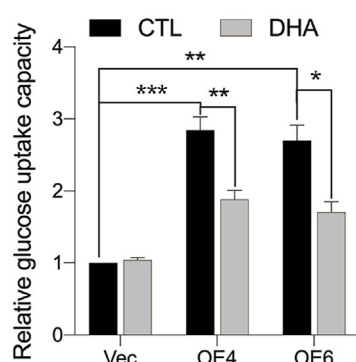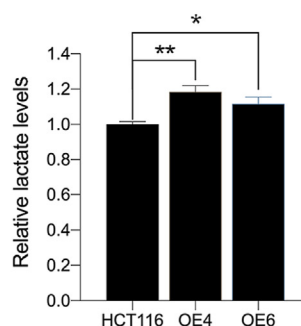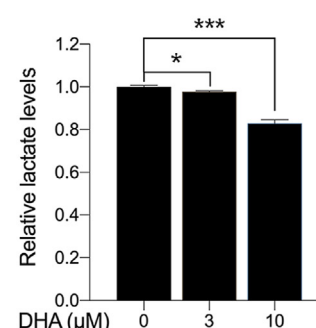| Compound, IC$_{50}$ (μM)	Vec	OE4	OE6
Canagliflozin	24.83 ± 1.19	29.43 ± 1.08*	32.38 ± 0.79**
WZB117	> 30	> 30	> 30
DHA	1.59 ± 0.07	0.69 ± 0.14**	0.75 ± 0.17**

Fig. 2. DHA selectively targets colorectal CSC-like cells which is in part associated with glucose metabolism. (A) The IC$_{50}$ values of glucose transporter inhibitors and DHA in Vec, OE4 and OE6 cells. The SRB assay was performed after 72 h of drug treatment to determine cell viability and calculate IC$_{50}$ values. DHA was more effective toward colorectal CSC-like OE4 and OE6 cells. *P < 0.05, **P < 0.01 vs. Vec. (B) Quantitative results of the sphere formation assay in HCT116, Vec, OE4 and OE6 cells treated with 50% inhibitory concentrations of DHA. (C) Glucose uptake capacity measured by 2-NBDG uptake and flow cytometric analysis. Compared to Vec, OE4 and OE6 cells had a higher glucose uptake capacity which was suppressed after 48 h of treatment with 2 × 50% inhibitory concentrations of DHA. (D) Relative lactate levels in culture media of HCT116, OE4 and OE6 cells. (E) Relative lactate levels in culture media of OE4 cells treated with 3 and 10 μM DHA for 48 h. CTL: vehicle control. *P < 0.05, **P < 0.01, ***P < 0.001.

Altogether, these results indicated that DHA preferentially suppressed the growth and stemness of CSC-like cell clones OE4 and OE6, and interruption of glucose metabolism may be one of the underlying mechanisms.

3.3. The effect of DHA on cell cycle progression and apoptosis in HCT116 and GATA6-overexpressing OE4 and OE6 cells

For further investigation of mechanisms of action, DHA concentrations higher than the IC$_{50}$ values at 72 h were used to observe changes at earlier time points. To evaluate the effect of DHA on cell cycle progression and apoptosis, HCT116, OE4 and OE6 cells were treated with 3 and 10 μM DHA for 24 and 48 h, followed by PI staining and flow cytometric analysis. In HCT116 cells, DHA significantly increased subG1 populations at 48 h (4.22 ± 0.66% by 3 μM and 6.84 ± 1.68% by 10 μM DHA compared to 1.11 ± 0.05% in the vehicle control, CTL) and G0/G1 populations at both 24 and 48 h. In contrast, the S and G2/M populations were significantly decreased at both time points (Fig. 3A). In OE4 cells, the subG1 population was augmented to a greater extent: 13.9 ± 2.34% by 3 μM and 16.2 ± 2.91% by 10 μM DHA at 24 h compared to 7.52 ± 1.17% in CTL; 21.8 ± 3.58% by 3 μM and 16.9 ± 2.90% by 10 μM DHA at 48 h compared to 5.59 ± 2.08% in CTL. Unlike in HCT116 cells, G0/G1 cells were slightly
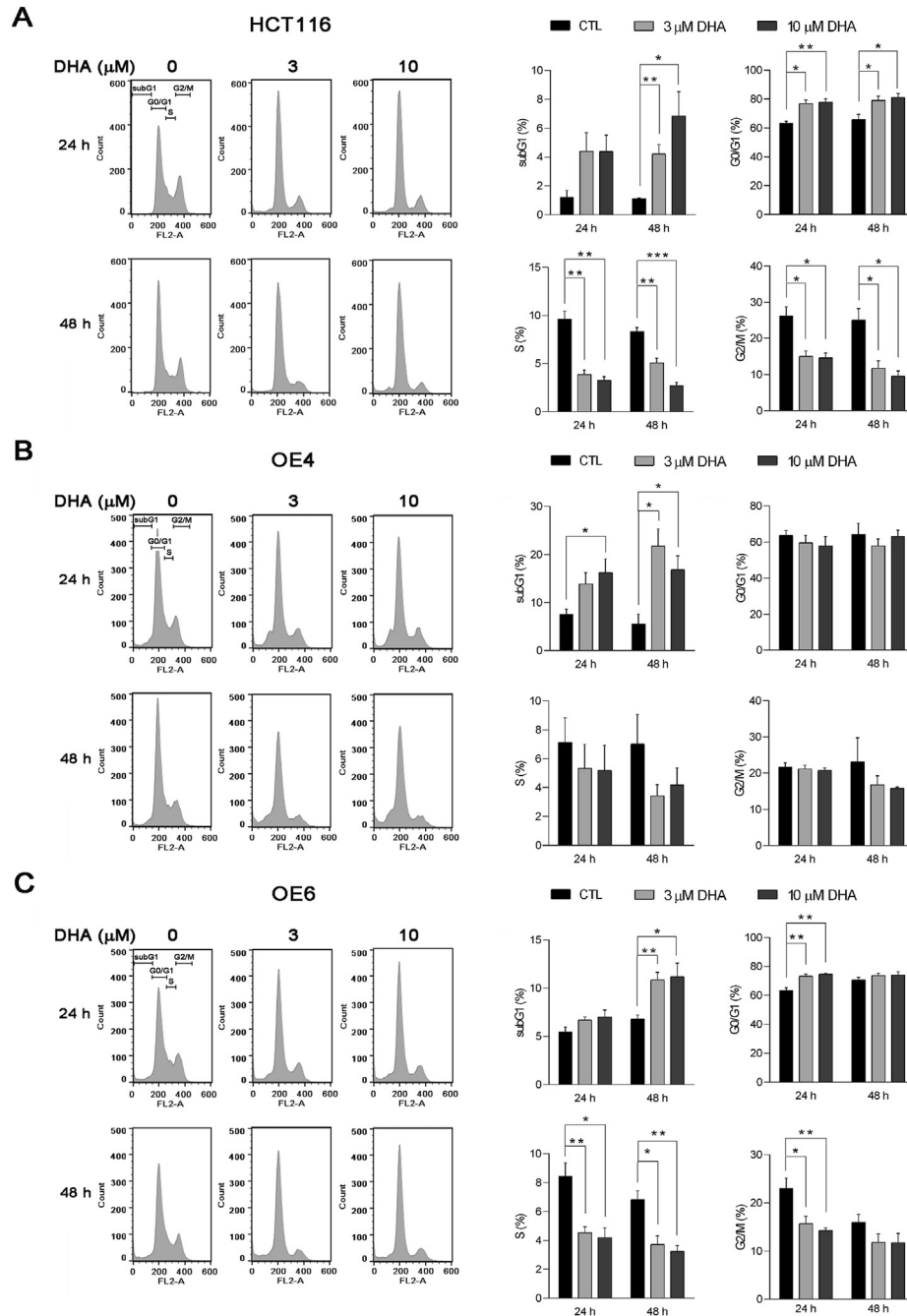
Fig. 3. The effect of DHA on cell cycle progression of HCT116 and GATA6-overexpressing OE4 and OE6 cells. (A) HCT116 cells. (B) OE4 cells. (C) OE6 cells. Cells were treated with 3 and 10 μM DHA for 24 and 48 h, and then harvested for PI staining and flow cytometric analysis. Representative cell cycle histograms are shown on the left and quantitative results are shown on the right. *P < 0.05, **P < 0.01, ***P < 0.001.

decreased at both 24 and 48 h by DHA in OE4 cells possibly due to more pronounced increases in subG1 populations. The S and G2/M populations had a similar decreasing trend as in HCT116 cells but without statistical significance (Fig. 3B). In OE6 cells, both 3 and 10 μM DHA significantly increased subG1 populations at 48 h (10.9 ± 0.78% and 11.2 ± 1.41% respectively compared to 6.81% ± 0.40

in CTL) and G0/G1 cells at 24 h, suggesting a transition from cell cycle arrest to apoptosis. Furthermore, DHA significantly decreased S phase cells at both time periods and G2/M populations at 24 h (Fig. 3C). Interestingly, OE cell clones showed higher subG1 populations than HCT116 cells even without drug treatment, indicating that there were more apoptotic cells in these CSC-like cells under

normal conditions. DHA also induced more subG1 cells in OE cell clones compared to HCT116 cells (Fig. 3).

To confirm that DHA induced cell apoptosis, Western blot analysis was conducted using HCT116, OE4 and OE6 cells treated with 3 or 10 μM DHA for 24 or 48 h. As shown in Fig. 4, DHA markedly induced cleaved PARP, a marker of apoptosis. Together, these results indicated that DHA may cause G0/G1 arrest and subsequently induce apoptosis in both HCT116 cells and CSC-like OE cell clones, and the induction of apoptosis was much more effective in colorectal CSC-like cells.

3.4. The effect of DHA on ROS induction in HCT116 and GATA6-overexpressing OE4 and OE6 cells

It is well-known that DHA can induce ROS production due to its endoperoxide moiety [12,13]. Thus, DCFH-DA assay was conducted to investigate the effect of DHA on ROS production. As shown in Fig. 5A, treatment with 10 μM DHA for 8 h significantly induced ROS production in HCT116 cells (geomean: 13.2 ± 0.24 vs. 9.23 ± 0.47 in CTL), OE4 cells (geomean: 22.0 ± 0.15 vs. 16.8 ± 1.14 in CTL) and OE6 cells (geomean: 23.2 ± 0.90 vs. 16.6 ± 0.90 in CTL). ROS induction by DHA was slightly reduced at 24 h. Notably, OE4 and OE6 cells had significantly higher basal ROS levels than HCT116 cells as shown in CTLs ($P < 0.05$).

Taken together, the results demonstrated that cellular ROS may be involved in the anticancer activity of DHA in colorectal CSCs. However, relatively higher basal ROS levels in OE4 and OE6 compared to HCT116 cells suggested that a slightly higher ROS level may also play a role in the stemness maintenance of these CSC-like cells.

3.5. The effect of DHA on mitochondrial dysfunction in HCT116 and GATA6-overexpressing OE4 and OE6 cells

Because DHA induced ROS production, we then investigated whether DHA caused the depolarization of mitochondrial membrane potential (MMP) using the JC-1 assay after 24 and 48 h of treatment. As shown in Fig. 5B, 3 μM DHA increased MMP loss at both 24 and 48 h. The induction of MMP loss by DHA was more significant at 48 h relative to the controls in HCT116 ($10.8 \pm 1.35\%$ vs. $2.93 \pm 0.03\%$ in CTL), OE4 ($21.7 \pm 2.25\%$ vs. $9.84 \pm 1.33\%$ in CTL) and OE6 ($28.3 \pm 2.17\%$ vs. $10.3 \pm 1.49\%$ in CTL) cells. Moreover, the percentages of MMP loss in OE clones were significantly higher than HCT116 cells in the control groups at both 24 and 48 h ($P < 0.01$).

To further examine the effect of DHA on mitochondrial function, Seahorse mitochondrial stress test assay was conducted. As shown in Fig. 5C, after treated with 3 μM DHA for 24 h, the oxygen consumption rate (OCR) showed similar profiles after adding oligomycin, FCCP and antimycin A/rotenone sequentially in HCT116 and OE cells. Notably, OCR tended to be higher in OE clones than HCT116 cells. The basal respiration, ATP production and maximal respiration of mitochondria were all significantly suppressed in HCT116 cells and OE clones (Fig. 5D). These results indicated that DHA affected the function of mitochondria in many aspects, suggesting that mitochondrial damage caused by DHA may be a potential anti-CSC mechanism.
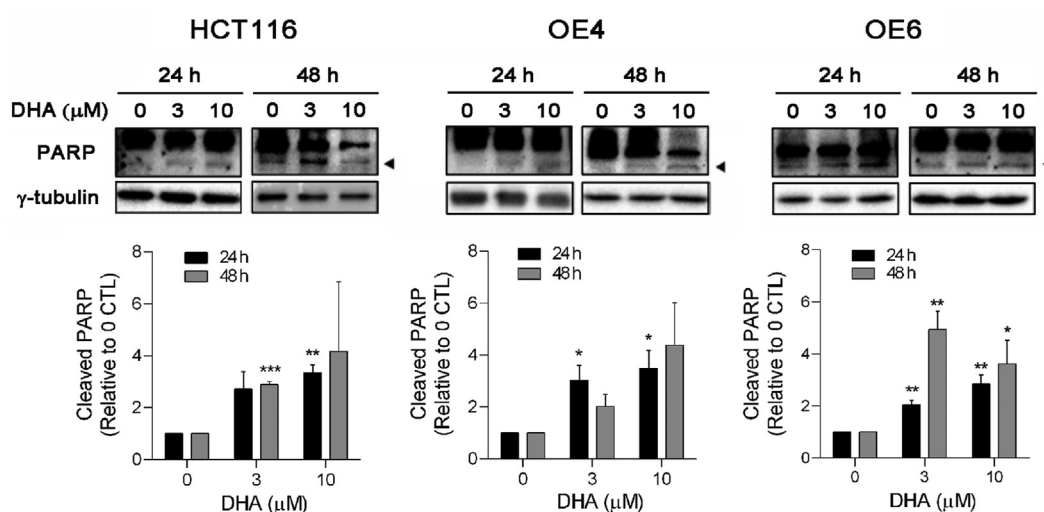

Fig. 4. DHA induces apoptosis in HCT116, OE4 and OE6 cells. Cells were treated with DHA for 24 and 48 h, then harvested for SDS-PAGE and Western blot analysis. Cleaved PARP is indicated with an arrowhead. *P < 0.05, **P < 0.01, ***P < 0.001 vs. respective untreated control.
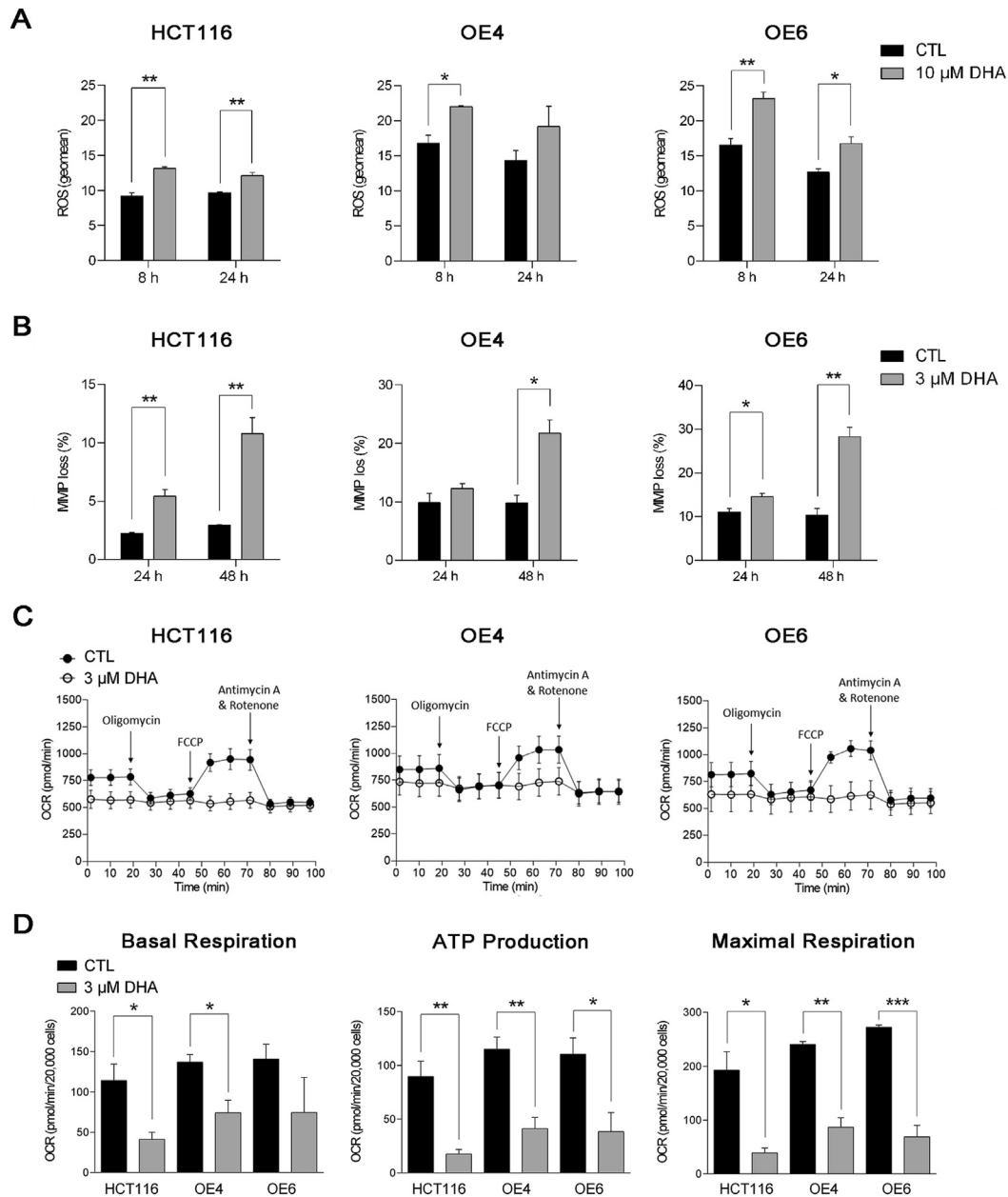
Fig. 5. DHA induces ROS, MMP loss and causes mitochondrial dysfunction in HCT116, OE4 and OE6 cells. (A) DHA induced ROS. Cells were treated with 10 μM DHA for 8 and 24 h, then subjected to the DCFH-DA assay. (B) DHA induced MMP loss. Cells were treated with 3 μM DHA for 24 and 48 h, then subjected to the JC-1 assay. (C) DHA suppressed OCR. Cells were treated with 3 μM DHA for 24 h and then subjected to the Seahorse mitochondrial stress test assay. (D) Quantitative results of basal respiration, ATP production and maximal respiration of mitochondria obtained from the Seahorse mitochondrial stress test. *P < 0.05, **P < 0.01, ***P < 0.001.

3.6. The effect of DHA on cancer stemness and autophagy/mitophagy markers in HCT116 and GATA6-overexpressing OE4 and OE6 cells

As mentioned above, DHA significantly affected the stemness (Fig. 2B) and function of mitochondria in HCT116 cells and OE clones (Fig. 5). Therefore, Western blot analysis of stemness-related proteins GATA6 and Nanog, as well as autophagy/

mitophagy-related proteins LC3B and PINK1 was conducted to verify the effects of DHA. Interestingly, GATA6 protein was clearly induced in HCT116 cells treated with 3 or 10 μM DHA for 24 h, but barely detectable at 48 h (Fig. 6A). In contrast, GATA6 was significantly downregulated in both OE4 and OE6 cells after 24 and 48 h of treatment with DHA (Fig. 6B–C), which may in part account for suppression of cancer stemness. Nanog was slightly
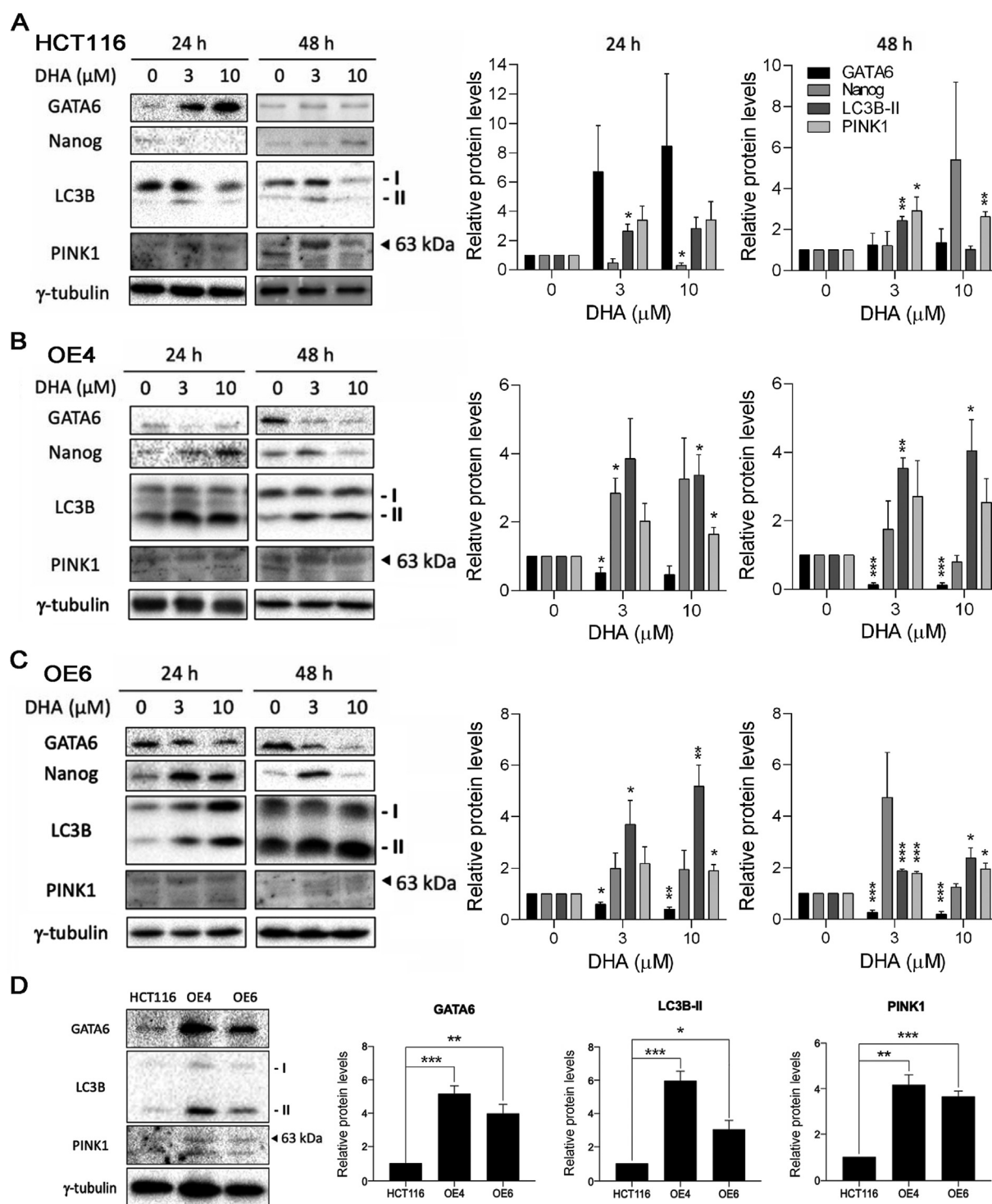
*Fig. 6. DHA downregulates GATA6 and induces autophagy/mitophagy markers in GATA6-overexpressing colorectal CSC-like cells. Western blot analysis of stem cell and autophagy/mitophagy markers in HCT116 (A), OE4 (B) and OE6 (C). Form I and form II of LC3B are indicated and the 63 kDa PINK1 bands are marked with arrowheads. (D) LC3B form II and PINK1 protein levels are higher in GATA6-overexpressing OE4 and OE6 than in HCT116 cells. *P < 0.05, **P < 0.01, ***P < 0.001.*

downregulated at 24 h and upregulated at 48 h by DHA in HCC116 cells (Fig. 6A). Surprisingly, Nanog was upregulated by both 3 and 10 μM DHA at 24 h which diminished at 48 h in OE4 and OE6 cells

(Fig. 6B—C). Similar trends of two other stem cell markers Oct4 and Sox2 were observed in OE4 cells treated with DHA as shown in Fig. S1 (Supplementary data https://doi.org/10.38212/2224-6614.3552).

In autophagy/mitophagy-related proteins, both LC3B-II and PINK1 were induced by DHA in HCT116, OE4 and OE6 cells, indicating that autophagy/mitophagy may be related to DHA-induced mitochondrial damage and contributed to cell death (Fig. 6A–C). Intriguingly, the basal protein levels of LC3B-II and PINK1 were significantly higher in GATA6-overexpressing OE4 and OE6 cell clones than in HCT116 cells (Fig. 6D). Together, these data suggested that slight elevation of autophagy and mitophagy in OE clones may help maintain stemness, while further elevation of autophagy and mitophagy induced by DHA may be associated with the growth inhibitory effect and/or cell death of colorectal CSCs.

3.7. Inhibition of autophagy attenuates DHA-induced apoptosis in HCT116 and GATA6-overexpressing OE4 and OE6 cells

To further clarify the effect of autophagy on colorectal CSCs, chloroquine, an autophagy inhibitor, was used to suppress the induction of autophagy by DHA. As shown in Fig. 7A, 10 μM chloroquine alone significantly suppressed the growth of all cells, suggesting that autophagy was cytoprotective. In contrast, chloroquine reversed the growth inhibitory effect of DHA in HCT116 cells and OE clones, but to a greater extent in OE clones, indicating that autophagy induced by DHA was associated with growth inhibition and cell death which was more prominent in colorectal CSC-like OE cells. Western blot analysis revealed that indeed PARP cleavage induced by DHA was significantly reversed by chloroquine in OE clones treated for 48 h (Fig. 7B–C). Surprisingly, in spite of suppressing cell growth (Fig. 7A), chloroquine alone significantly reduced cleaved PARP in HCT116 cells after 48 h of treatment (Fig. 7C), reflecting the complexity of autophagy. The levels of LC3B-II were even higher after the combination of DHA with chloroquine as expected due to the effect of chloroquine (Fig. 7B).

4. Discussion

Although CSCs are only a small subpopulation within total cancer cells, they account for tumorigenesis, cancer progression, metastasis and drug resistance, thus have been considered good targets for cancer therapy. Three-dimensional culture methods such as sphere formation assay and organoid culture are usually used to enrich and maintain long-term stemness of CRCs. Since defined serum-free culture media and/or Matrigel are used in these culture methods, they may not

be convenient and cost-effective platforms for the screening of CSC-targeting agents. GATA6-overexpressing HCT116 cell clones established previously [7] displayed CSC-like properties and could be a convenient and cost-effective colorectal CSC-like cell model for the identification of colorectal CSC-targeting agents since these cell clones can be maintained in serum-containing medium using the regular 2-D cell culture system.

Many studies have revealed that DHA exhibits anticancer activity in a wide variety of cancers including lung, breast, pancreatic, prostate, ovarian and colorectal cancers [12]. Moreover, a few studies have also demonstrated that DHA displays an inhibitory effect on cancer stemness toward glioma [13], lung cancer [18], laryngeal carcinoma [19], and colorectal cancer [20,21]. We characterized and verified GATA6-overexpressing HCT116 cell clones OE4 and OE6 as a colorectal CSC-like cell model by sphere formation assay, Western blot analysis of stemness-related proteins, determination of resistance to standard chemotherapy, and staining of CSC surface markers. Using this colorectal CSC-like cell model, we demonstrated for the first time that DHA preferentially targeted colorectal CSCs. CSCs are considered the main cause of drug resistance in CRC [17] and less vulnerable to chemotherapeutic drugs. Our colorectal CSC-like GATA6-overexpressing HCT116 cell clones OE4 and OE6 were less sensitive to 5-FU (Fig. 1C) as expected, but at least two times more sensitive to DHA than HCT116 cells transfected with an empty vector (Fig. 2A). Results from the sphere formation assay confirmed that DHA was able to suppress cancer stemness of HCT116 cells, and this effect was more effective toward CSC-like OE4 and OE6 cell clones (Fig. 2B) which may in part due to downregulation of GATA6 (Fig. 6B–C).

Significant increases in subG1 and G0/G1 cell populations were found in DHA-treated HCT116 and OE6 cells, whereas no clear increases in G0/G1 populations were observed in DHA-treated OE4 cells which could be due to more profound induction of subG1 cells since cells arrest at G0/G1 may subsequently undergo apoptosis and become the subG1 population (Fig. 3). Thus, DHA might induce G0/G1 arrest followed by apoptosis, which was confirmed by increased levels of cleaved PARP (Fig. 4). Alternatively, DHA may simply enhance apoptosis and further analysis is warranted. It has been reported that DHA induced G1 cell cycle arrest, apoptotic cell death and accumulation of ROS in HCT116 cells [20]. We also observed that DHA increased cellular ROS levels (Fig. 5A) likely via the cleavage of its endoperoxide bridge, which
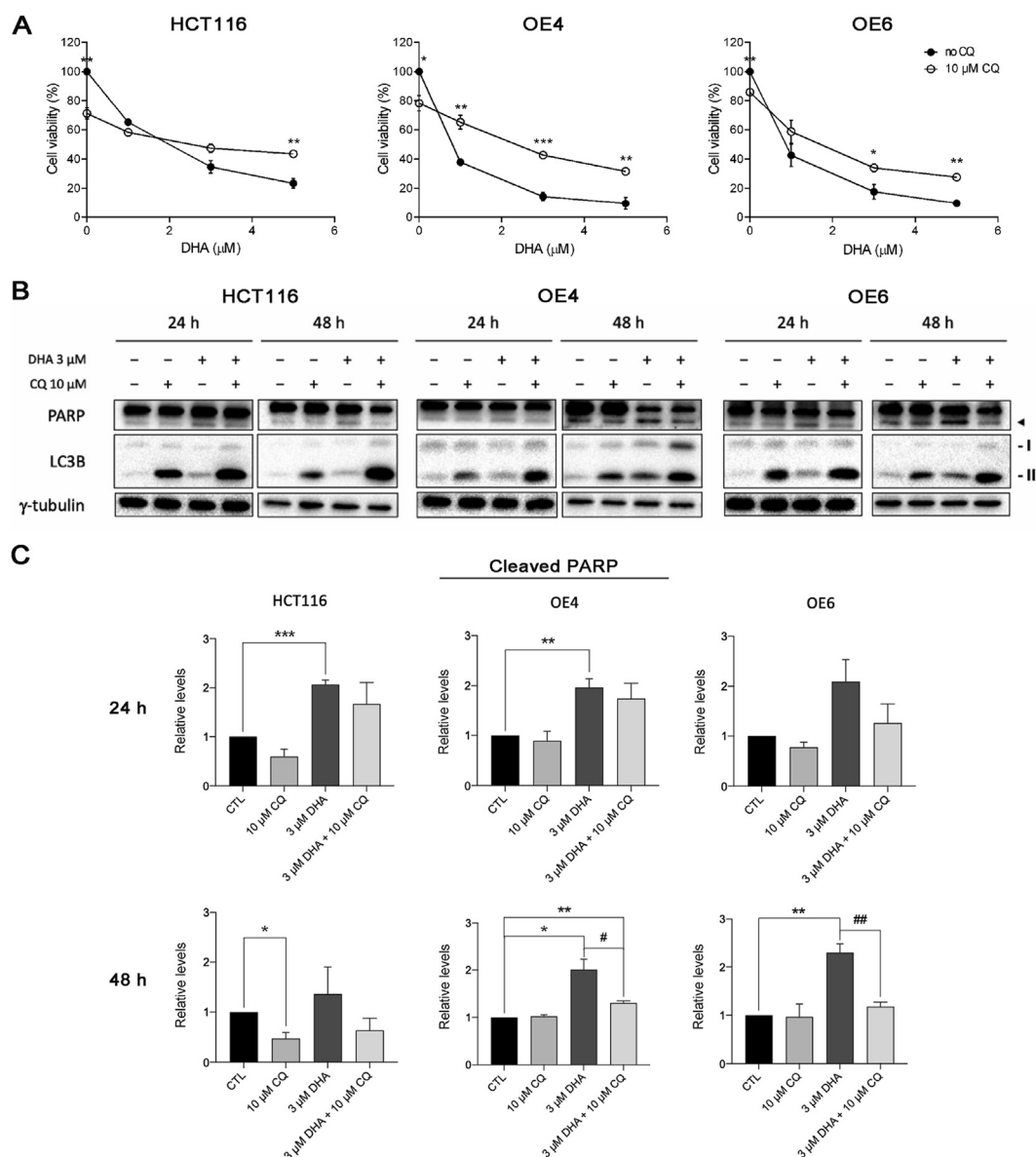
Fig. 7. Inhibition of autophagy attenuates DHA-induced apoptosis in HCT116, OE4 and OE6 cells. (A) Inhibition of autophagy by chloroquine (CQ) decreased cell survival but significantly reversed the growth inhibitory effect of DHA. Cells were treated with DHA in the absence or presence of 10 μM CQ for 72 h followed by the SRB assay to measure cell viability. (B) CQ reversed apoptosis induced by DHA. Cells were treated for 24 and 48 h, then harvested for Western blot analysis. Cleaved PARP is marked by an arrowhead, Form I and form II of LC3B are indicated. (C) Quantitative results of cleaved PARP. *P < 0.05, **P < 0.01, ***P < 0.001 vs. CTL. #P < 0.05, ##P < 0.01, DHA vs. DHA + CQ.

may subsequently lead to MMP loss (Fig. 5B), mitochondrial dysfunction (Fig. 5C–D) and eventually apoptosis (Fig. 4). It has been demonstrated that elevated mitochondrial ROS levels in a murine mammary tumor cell line and three human CRC cell lines were associated with higher tumor-initiating ability and metastatic potential [22]. On the other hand, it has also been reported that breast CSC-enriched populations had lower ROS levels, which was associated with increased expression of free radical scavenging genes [23]. Such controversial findings could be in part due to different types of cancer cells used. Hence, the association between the ROS levels and cancer stemness required further clarifications. We found that the basal levels of ROS were higher in colorectal CSC-like OE clones than in the parental HCT116 cells (Fig. 5A), suggesting that ROS may play a role in maintaining stemness of CRC cells. Indeed, ROS could drive stem cell expansion in CRC through functioning as signaling molecules [24]. Furthermore, it was demonstrated that antioxidants N-acetylcysteine and ascorbic acid dramatically reduced the self-renewal ability of colorectal CRCs

[25]. Thus, ROS levels are critical for survival of CSCs and DHA may also disturb the survival of CSCs by inducing the accumulation of ROS.

Excess accumulation of ROS may cause mitochondrial permeability transition pore openings and damage mitochondria [26]. Unlike cancer cells mainly relying on aerobic glycolysis to provide energy and building blocks of biomolecules, CSCs can be highly glycolysis or oxidative phosphorylation-dependent. Thus, mitochondrial function is critical for CSCs [27]. We found that DHA increased MMP loss (Fig. 5B), and inhibited basal respiration, ATP production and maximal respiration of mitochondria in HCT116 cells and OE clones (Fig. 5C–D), indicating that DHA caused mitochondrial damage in colorectal CSCs. As shown in Fig. S1 (Supplementary data https://doi.org/10.38212/2224-6614.3552), cytochrome c oxidase subunit 4 (COXIV), a component of the cytochrome c oxidase (also called complex IV) in the mitochondrial electron transport chain which drive oxidative phosphorylation, was downregulated by DHA in OE4 cells, suggesting that DHA may inhibit mitochondrial respiration through inhibition of electron transport chain. Artesunate, another artemisinin derivative has been reported to induce mitochondrial dysfunction leading to selective inhibition of stemness in induced cancer stem cell-like (iCSCL) cells iCSCL-10A established from an immortalized normal human mammary epithelial cell line MCF-10A by the iPS technology [28]. Taken together, DHA may suppress the mitochondrial function of colorectal CSCs by causing accumulation of excessive ROS resulting in inhibition of cancer stemness.

Mitophagy, the selective removal of damaged mitochondria by autophagy, is often considered a prosurvival pathway and has been reported to maintain the stemness of CSCs [29,30]. GATA6 can upregulate autophagy and confer tyrosine kinase inhibitor resistance in non-small cell lung cancer [31]. Here we found that GATA6 may also upregulate autophagy in colorectal CSC-like OE4 and OE6 cells which showed higher protein levels of LC3B-II, a marker of autophagy, than the parental HCT116 cells (Fig. 6D). After DHA treatment, protein levels of LC3B-II and PINK1, a kinase associated with mitophagy, were both significantly elevated, suggesting that DHA induced both autophagy and mitophagy. DHA has been reported to induce autophagy, which may lead to cell death [13]. Autophagy/mitophagy could be cytoprotective or cytotoxic depending on cellular contexts. Using a well-known autophagy inhibitor chloroquine, we found that growth inhibition and induction of apoptosis by DHA was more significantly reversed

by chloroquine in colorectal CSC-like OE clones than in the parental HCT116 cells (Fig. 7), suggesting that autophagy/mitophagy induced by DHA was associated with cytotoxicity in colorectal CSC-like OE clones. Interestingly, autophagy was cytoprotective in HCT116 and OE cells without DHA treatment as revealed by clear decreases in cell viability when treated with chloroquine alone (Fig. 7A). However, chloroquine alone did not increase cleaved PARP (Fig. 7B–C), suggesting that the concentration of chloroquine used in this study (10 μM) may only suppress cell growth but may not be sufficient to induce apoptosis in HCT116 and OE cells. Our data indicate that DHA may suppress stemness and cell survival of colorectal CSCs in part by induction of autophagy/mitophagy. However, further investigation is required to clarify the effect of autophagy/mitophagy more comprehensively.

Intriguingly, GATA6 protein levels were elevated dramatically at 24 h but dropped down to levels close to the untreated control at 48 h in HCT116 cells treated with 3 and 10 uM DHA (Fig. 6A). Furthermore, increased Nanog levels were observed in OE4 and OE6 cells treated with DHA for 24 h; however, Nanog protein levels diminished after 48 h of treatment with 10 μM DHA (Fig. 6B–C). It was unclear why the levels of these stem cell markers were increased at 24 h, but the protein levels diminished at 48 h which is likely to be correlated with the inhibitory effect of DHA on cancer stemness. It has also been reported that DHA inhibited stem cell-like properties and significantly downregulated Nanog in HCT116 cells treated with 20–40 μM DHA for 72 h [21]. GATA6 protein levels were downregulated by DHA at both 24 and 48 h in OE4 and OE6 cells (Fig. 6B–C). It was demonstrated that ROS-induced GATA4 and GATA6 downregulation inhibited the expression of progesterone synthesis-associated genes in lipopolysaccharide-treated porcine granulosa-lutein cells, an in vitro-luteinized granulosa cell model [32]. Thus, we speculated that DHA may downregulate GATA6 through induction of excess ROS in OE cells. Future work is needed to shed light on the exact mechanism by which DHA downregulates GATA6.

Subedi et al. have demonstrated the CSC-targeting ability of artesunate through high throughput screening and reported that the targeting ability of artesunate may involve mitochondrial metabolism [28]. Previous studies have also shown that GATA6 enhances stemness of human CRC cells via creating a metabolic symbiosis between CSC subpopulations favoring glycolysis and oxidative phosphorylation, respectively, suggesting that simultaneously targeting glycolysis and mitochondrial metabolism could be the

best approach to eradicate colorectal CSCs [25]. Here we found that DHA targeted CSC-like GATA6-over-expressing HCT116 cells not only by inhibition of glucose uptake and glycolysis (Fig. 2C—E), but also by impairment of mitochondrial function (Fig. 5) leading to autophagy/mitophagy-associated apoptosis which was reversed by an autophagy inhibitor chloroquine (Fig. 7).

In summary, we verified a colorectal CSC-like cell model and applied it to identify DHA as a colorectal CSC-targeting compound. Mechanistic studies revealed that the anti-CSC activity of DHA was associated with inhibition of glucose uptake and glycolysis, and induction of ROS, MMP loss and autophagy/mitophagy, and finally leading to apoptosis. The clinical median DHA Cmax was reported to be 3140 ng/mL (11 μM) and the range was 1670—9530 ng/mL (5.9—33.5 μM), which did not cause adverse events for the treatment of severe malaria [33]. Therefore, the highest concentration used in our studies (10 μM) should be clinically relevant. Thus, DHA can be repurposed as an effective drug to target CSCs of CRC and maybe other cancer types as well. Studies using different cell lines or organoids derived from patients are needed to further validate the effects of DHA. In addition, since the behavior of CSCs is highly influenced by tumor microenvironment, future investigation in xenograft and/or orthotopic mouse models to provide *in vivo* evidence is warranted.

Conflicts of interest

The authors declare no conflict of interest.

Acknowledgments

References

[1] Bray F, Laversanne M, Sung H, Ferlay J, Siegel RL. Global cancer statistics 2022: GLOBOCAN estimates of incidence and mortality worldwide for 36 cancers in 185 countries. CA Cancer J Clin 2024;74:229—63.
[2] American Cancer Society. Survival rates for colorectal cancer. Available from: https://www.cancer.org/cancer/types/colon-rectal-cancer/detection-diagnosis-staging/survival-rates.html.
[3] Biller LH, Schrag D. Diagnosis and treatment of metastatic colorectal cancer: a review. JAMA 2021;325:669—85.
[4] Yang L, Shi P, Zhao G, Xu J, Peng W, Zhang J, et al. Targeting cancer stem cell pathways for cancer therapy. Signal Transduct Targeted Ther 2020;5:8.
[5] Beuling E, Aronson BE, Tran LMD, Stapleton KA, ter Horst EN, Vissers LATM, et al. GATA6 is required for proliferation, migration, secretory cell maturation, and gene expression in the mature mouse colon. Mol Cell Biol 2012;32:3392—402.
[6] Tsuji S, Kawasaki Y, Furukawa S, Taniue K, Hayashi T, Okuno M, et al. The miR-363-GATA6-Lgr5 pathway is critical for colorectal tumourigenesis. Nat Commun 2014;5:3150.
[7] Lai HT, Tseng WK, Huang AW, Chao TC, Su Y. MicroRNA-203 diminishes the stemness of human colon cancer cells by suppressing GATA6 expression. J Cell Physiol 2020;235:2866—80.
[8] Du FY, Zhou QF, Sun WJ, Chen GL. Targeting cancer stem cells in drug discovery: current state and future perspectives. World J Stem Cell 2019;11:398—420.
[9] Shibuya K, Okada M, Suzuki S, Seino M, Seino S, Takeda H, et al. Targeting the facilitative glucose transporter GLUT1 inhibits the self-renewal and tumor-initiating capacity of cancer stem cells. Oncotarget 2015;6:651—61.
[10] Basak D, Gamez D, Deb S. SGLT2 inhibitors as potential anticancer agents. Biomedicines 2023;11:1867.
[11] Tu Y. The discovery of artemisinin (qinghaosu) and gifts from Chinese medicine. Nat Med 2011;17:1217—20.
[12] Zhang Y, Xu G, Zhang S, Wang D, Saravana Prabha P, Zuo Z. Antitumor research on artemisinin and its bioactive derivatives. Nat Prod Bioprospect 2018;8:303—19.
[13] Xu C, Zhang H, Mu L, Yang X. Artemisinins as anticancer drugs: novel therapeutic approaches, molecule mechanisms, and clinical trials. Front Pharmacol 2020;11:529881.
[14] Cao L, Duanmu W, Yin Y, Zhou Z, Ge H, Chen T, et al. Dihydroartemisinin exhibits anti-glioma stem cell activity through inhibiting p-AKT and activating caspase-3. Pharmazie 2014;69:752—8.
[15] Huang H, Kung FL, Huang YW, Hsu CC, Guh JH, Hsu LC. Sensitization of cancer cells to paclitaxel-induced apoptosis by canagliflozin. Biochem Pharmacol 2024;223:116140.
[16] Kao TY, Wu HW, Lee SS, Liang PH, Guh JH, Hsu LC. Characterization of a fluorescent glucose derivative 1-NBDG and its application in the identification of natural SGLT1/2 inhibitors. J Food Drug Anal 2021;29:521—32.
[17] Das PK, Islam F, Lam AK. The roles of cancer stem cells and therapy resistance in colorectal carcinoma. Cells 2020;9:1392.
[18] Tong Y, Liu Y, Zheng H, Zheng L, Liu W, Wu J, et al. Artemisinin and its derivatives can significantly inhibit lung tumorigenesis and tumor metastacis through Wnt/β-catenin signaling. Oncotarget 2016;7:31413—28.
[19] Wang W, Sun Y, Li X, Shi X, Li Z, Lu X. Dihydroartemisinin prevents distant metastasis of laryngeal carcinima by inactivating STAT3 in cancer stem cells. Med Sci Monit 2020;26:e922348.
[20] Lu M, Sun L, Zhou J, Yang J. Dihydroartemisinin inuces apoptosis in colorectal cancer cells through the mitochondria-dependent pathway. Tumor Biol 2014;35:5307—14.
[21] Wang Y, Yang Z, Zhu W, Chen Y, He X, Li J, et al. Dihydroartemisinin inhibited stem cell-like properties and enhanced oxaliplatin sensitivity of colorectal cancer via AKT/mTOR signaling. Drug Dev Res 2023;84:988—98.
[22] Wang C, Shao L, Pan C, Ye J, Ding Z, Wu J, et al. Elevated level of mitochondrial reactive oxygen species via fatty acid β-oxidation in cancer stem cells promotes cancer metastasis by inducing epithelial-mesenchymal transition. Stem Cell Res Ther 2019;10:175.
[23] Diehn M, Cho RW, Lobo NA, Kalisky T, Dorie MJ, Kulp AN, et al. Association of reactive oxygen species levels and radioresistance in cancer stem cells. Nature 2009;458:780—3.

[24] Pelicci PG, Dalton P, Giorgio M. The other face of ROS: a driver of stem cell expansion in colorectal cancer. Cell Stem Cell 2013;12:635−6.

[25] Lai HT, Chiang CT, Tseng WK, Chao TC, Su Y. GATA6 enhances the stemness of human colon cancer cells by creating a metabolic symbiosis through upregulating *LRH-1* expression. Mol Oncol 2020;14:1327−47.

[26] Zorov DB, Juhaszova M, Sollott SJ. Mitochondrial reactive oxygen species (ROS) and ROS-induced ROS release. Physiol Rev 2014;94:909−50.

[27] Sancho P, Barneda D, Heeschen C. Hallmarks of cancer stem cell metabolism. Br J Cancer 2016;114:1305−12.

[28] Subedi A, Futamura Y, Nishi M, Ryo A, Watanabe N, Osada H. High-throughput screening identifies artesunate as selective inhibitor of cancer stemness: involvement of mitochondrial metabolism. Biochem Biophys Res Commun 2016; 477:737−42.

[29] Liu K, Lee J, Kim JY, Wang L, Tian Y, Chan S, et al. Mitophagy controls the activities of tumor suppressor p53 to regulate hepatic cancer stem cells. Mol Cell 2017;68: 281−92.

[30] Panigrahi DP, Praharaj PP, Bhol CS, Mahapatra KK, Patra S, Behera BP, et al. The emerging, multifacted role of mitophagy in cancer and cancer therapeutics. Semin Cancer Biol 2020;66:45−58.

[31] Ma R, Li X, Liu H, Jiang R, Yang M, Zhang M, et al. GATA6-upregulating autophagy promotes TKI resistance in nonsmall cell lung cancer. Cancer Biol Ther 2019;20: 1206−12.

[32] Qu X, Yan L, Guo R, Li H, Shi Z. ROS-induced GATA4 and GATA6 downregulation inhibits StAR expression in LPS-treated porcine granulosa-lutein cells. Oxid Med Cell Longev 2019;2019:5432792.

[33] Byakika-Kibwika P, Lamorde M, Mayito J, Nabukeera L, Mayanja-Kizza H, Katabira E, et al. Pharmacokinetics and pharmacodynamics of intravenous artesunate during severe malaria treatment in Ugadan adults. Malaria J 2012;11: 132.